Simple way to make Anatase TiO_2 films on FTO glass for promising solar cells

A.T.Raghavender [a,*] A. P. Samantilleke [b], Pedro Sa [b], B. G. Almeida [b], M. I. Vasilevskiy [b], Nguyen Hoa Hong [a]

[a] Nanomagnetism Laboratory, Department of Physics and Astronomy, Seoul National University, Seoul 151-747, South Korea

[b] Centro de Fısica, Universidade do Minho, Braga 4710 057, Portugal

Abstract

TiO_2 is a wide bandgap semiconductor material used as the photo anode in dye sensitized solar cells (DSSC). The fabrication of TiO_2 on conductive glass substrates plays an important role in the solar cell efficiency, since the thickness of the TiO_2 coating affects the transmission, photoconductive properties and the efficiency of solar cells. The uncorrected transmission in our fabricated films is as high as 80 %, and the bandgap obtained is similar to that of bulk anatase TiO_2, confirming that sol-gel prepared films in this work can be used effectively for DSSC.

Key words: TiO_2; structural; Optical properties

***Corresponding author:**

Telephone: +82-2-880-6606, Fax: +82-2-884-3002

Email: atraghavender@snu.ac.kr, raghavi9@gmail.com (A.T. Raghavender)

1. Introduction

Titanium dioxide (TiO_2) or titania has been a subject of interest for decades due to its chemical properties, such as stability and non-toxicity, as well as its physical properties such as high transmittance in the visible spectral region, wide bandgap, high refractive index and permittivity. Although, titania shows photocatalytic activity only under UV light irradiation, because of its wide bandgap ~ 3.0 eV for rutile and ~3.2 eV for anatase, it has been proven a good window material in photovoltaic applications. In fact, TiO_2 is extensively used in the applications of dye sensitized solar cells (DSSC) [1]. The anatase phase has been preferred for its photocatalytic properties and widely used in solar cell applications, primarily owing to its wider bandgap [2]. One most important requirement of widegap materials for the application of solar cells is to have maximum possible transmission. The optical properties and the electronic transport properties of TiO_2 thin films depend on the fabrication process and the phase of the material.

The sol gel technique has extensively been used together with doctor blade method to produce nanoparticle structures of wide bandgap materials. Some of the advantages of such methods include the ability to deposit pre-determined structures by varying experimental conditions, homogeneity, low temperature preparation and low production cost [3]. It is noteworthy that thin films and nano- and poly-crystalline samples deposited by sol gel method can have different characteristics of compositional distribution and phase stability. The solubility range of as-prepared thin films appears significantly wider than that in the crystalline phases, because thin-film growth processes are substantially affected by kinetic parameters. Other low-cost wet chemical techniques have also been successfully used in depositing wide

bandgap materials such as ZnO [4]. Straumal et al [4] used a dip coating method to deposit a nanocrystalline thin film in a mixture of liquid organic acids at 150ºC. Annealing at higher temperature (550ºC) has lead to grain growth. Thus in order to understand and to explore the fabrication process of nanocrystallineTiO_2 on fluorine- doped tin oxide (FTO) conducting glass for the applications in solar cells, we have investigated different properties which are presented in this paper. A simple low-cost and an efficient method for the deposition of anatase TiO_2 thin films were used in this work.

2. Experimental

The TiO_2 nanoparticles were prepared by a sol–gel method [5]. TiO_2 nonporous thin films on fluorine doped tin oxide (FTO) glass were fabricated using the doctor blade method. The structural characterization of the prepared thin films was carried out using a Bruker AXS D8 advanced high resolution X-ray diffractometer (HRXRD) (wavelength λ=1.542 Å). The morphology of powder and thin films was observed using a Hitachi SU-70, high resolution scanning electron microscope (HR-SEM). The transmission spectrum was measured using a Schimadzu UV-3101 PC spectrometer for optical characterization. The dielectric measurements were carried using a Wayne Kerr 6440A in the frequency range 20Hz-3MHz with Precision Component Analyzer. The sample set up was connected as a parallel plate capacitor.

3. Results and discussions

Fig.1 (a) shows the X-ray diffraction patterns of TiO_2 nanoparticles and TiO_2 coated on FTO glass. All the XRD peaks of TiO_2 clearly indicate the unique phase of anatase. The microstructure of the prepared anatase TiO_2 nanoparticles is shown in Fig.1(b). The HR-SEM

image clearly shows the nanocrystallinity of the samples. The cross-section and the plane view microstructure of TiO_2 coated on FTO glass is as shown in Fig. 1(c) and (d). The TiO_2 coating on FTO glass can be clearly seen in Fig.1(c). The plane view of the FTO/TiO_2 image (Fig.1(d)) shows the uniform distribution of the TiO_2 coating on the FTO glass.

Dielectric measurements at room temperature were performed for FTO/TiO_2 using a silver electrode at the top. Fig. 2 shows the variation of dielectric constant (ε') versus frequency. Generally, ε', decreases with increasing frequency. The value of the dielectric constant is very high at lower frequencies and decreases with increasing frequency. The higher values of ε' at lower frequencies were due to the simultaneous presence of space charge, dipolar, ionic, and electronic polarizations. At lower frequencies the grain boundaries are more effective than grain electrical conduction. The decrease in the ε' with increasing frequency can be explained on the basis of the mechanism of polarization process as in ferrites [6], which is similar to that in the conduction process [7]. The inset of Fig.2 shows the variation of dielectric loss tangent ($tan\ \delta$) and dielectric loss factor (ε'') with frequency for FTO/TiO_2 sample. The $tan\ \delta$ and the ε'' decrease rapidly at lower frequencies and then slowly at higher frequencies. Kramer and Panova [8] explain that the increase of loss factor at higher frequency would be attributed to the phenomenon of domain wall relaxation. The occurrence of high value of loss factor at lower frequency is due to the different types of wall relaxation processes [9]. The maximum loss occurs at a frequency $\tau = 1/\omega$, which is proportional to the conductivity [10]. Our observed variation appears to have a similar behavior.

Fig. 3 shows the measured transmittance (T) spectra of three TiO_2 thin films in the spectral region with interference fringes. One spectrum has two adjacent maxima and minima marked T_M and T_m respectively. Assuming the TiO_2 samples to be homogeneous and uniform,

thin films with thickness *d*, deposited on transparent substrates, whose thickness was several orders of magnitude larger than *d*, is given by the basic equation for the interference fringes:

$$2nd = m\lambda \qquad (1)$$

Here, n is the refractive index of TiO_2 and *m* takes the form of an integer for interference maxima and half integer for minima. Taking into account two adjacent maxima and a minimum (T_M and T_m), according to Swanepoel's method [11] following Aly et al[12], the thickness of the TiO_2 films (*d*), can be expressed as:

$$d = \frac{\lambda_1 \lambda_2}{2(n_1\lambda_2 - n_2\lambda_1)} \qquad (2)$$

where n_1 and n_2, are the refractive indices and λ_1 and λ_2 are the photon wavelengths of the adjacent maxima and minima as labeled in Fig.3. In these calculations, it was assumed that the refractive indices $n_1 = n_2 = n$. As described by Aly et al [12], the refractive index *n* in the spectral region of medium and weak absorption can be derived from the formula.

$$n = \sqrt{(N + \sqrt{N^2 - S^2})} \qquad (3)$$

where $N = 2S\frac{T_M - T_m}{T_M T_m} + \frac{1+S^2}{2}$

The refractive index of glass, *s* can be estimated from the equation (4)

$$S = \left(\frac{1}{\tau_S}\right) + \sqrt{\left(\frac{1}{\tau_S^2} - 1\right)} \qquad (4)$$

where τ_s is the measured glass transmittance [13]. The raw values of T_s and calculated S values that were used in the thickness calculation corresponding to λ_{max} are also given in Table 1.

The absorption coefficient (α) in the high-absorption region ($\alpha \geq 10^4$ cm^{-1}), is given by the Tauc equation (equation 5).

$$\alpha(\lambda) = \frac{B(h\nu - E_g)^2}{h\nu} \qquad (5)$$

where B, $h\nu$, and E_g are a parameter that depends on the transition probability, the photon energy and the optical bandgap respectively. The transmission data were used to derive α (α = -(1/d)lnT)and the Tauc plot ($(\alpha.h\nu)^{1/2}$ vs hν) for the three spectra A,B,C in Fig.3 are plotted in Fig.4.

Optical bandgaps E_g extrapolated using Tauc plot (Fig.4) for three samples considered are ~3.2 eV, which corresponds to an indirect transition and of almost the same as that of the bulk TiO_2 at room temperature. Usually, nanocrystalline anatase TiO_2 thin films show larger bandgap values than that of the bulks, presumably due to axial strain effects and furthermore, to the difference in the density of carriers [14]. A more accurate value for the bandgap may be achieved by including the loss factors due to scattering of light and considering more accurate refractive indices for maxima and minima. The films are of similar thickness, suggesting the method of deposition to produce consistently uniform thin films. However, as shown in Table 1, the refractive indices of the three samples at maxima are 2.14 (955 nm), 2.15 (963 nm) and 2.23 (945 nm), which are typical of TiO_2 at near infra-red wavelengths.

Conclusions:

Stable anatase TiO_2 nanoparticles were synthesized by using a low-temperature sol-gel method. Nanoporous thin films on fluorine doped tin oxide (FTO) glass were made by a conventional doctor blade method. XRD and HR-SEM analyses confirmed that the films were uniform and of anatase phase TiO_2 nanostructures (with ~30 nm particle size). The dielectric constant of TiO_2, was found to be very high at lower frequencies, and it decreases with increasing frequency. Optical transmission studies further confirm the bandgap of TiO_2 film to be similar to that of bulks. The transmission of our films could achieve as high as 80%. Optical constants derived from the transmission spectra are also typical of bulk TiO_2 at near infra-red wavelengths. TiO_2 films made by this simple method indeed can be used as a part of future solar cells.

Acknowledgements:

The authors would like to thank the grant EU-FT funded by NRF Korea for financial support and Prof. M. Fatima Cerqueira, Centro de Fısica, Universidade do Minho for providing experimental facilities. ATR thanks, "BK21 Frontier Physics Research Division, Department of Physics and Astronomy, Seoul National University, Seoul, South Korea" for the Postdoctoral fellowship. APS thanks Fundação para a Ciência e a Tecnologia (FCT), Portugal for funding.

References:

[1] Konstantinidis S, Dauchot J P, Hecq M. Thin Solid Films 2006; 515: 1182.

[2] Mills A, hunte S Le. J Photochem Photobiol A Chem 1997; 108: 1.

[3] Mackenzie J.M. J Non-Crstal Solids 1982; 48: 1.

[4] Straumal B. B, Mazilkin A A, Protasova S. G, Myatiev A A, Straumal P B, Baretzky B B. Acta Mater 2008; 56: 6246.

[5] Raghavender AT, Pajić D, Zadro K, Milekovi T, Venkateshwar Rao P, Jadhav KM, Ravinder D. J Magn Magn Mater 2007; 316: 1.

[6] Raghavender A T, Shirsath S E, Vijaya Kumar K. J Alloys Comp 2011; **509:** 7004.

[7] Abdul Gafoor A K, Thomas J, Musthafa M M, Pradyumnan P P, J Elect Mater 2011; 40: 2152.

[8] Kramer G P, Panova Y I. Phys Status Solidi A 1983; 77: 483.

[9] Smit J. Magnetic Properties of Materials, McGraw-Hill Co., NY, 1971.

[10] Babar V K, Chandal J S. Bull Mater Sci 1995; 18: 997.

[11] Swanepoel R. J Phys E: Sci Instrum 1983; 16: 1214.

[12] Aly K A, Amer H H, Dahshan A. Mater Chem Phys 2009; 113: 690.

[13] Jenkins F A, White H E. Fundamentals of Optics, McGraw-Hill, NewYork, 1957.

[14] Tanemura S, Miao L, Jin P, Kaneko K, Terai A, Nabatova-Gabain N. Appl Surface Sci 2003; 212–213: 654.

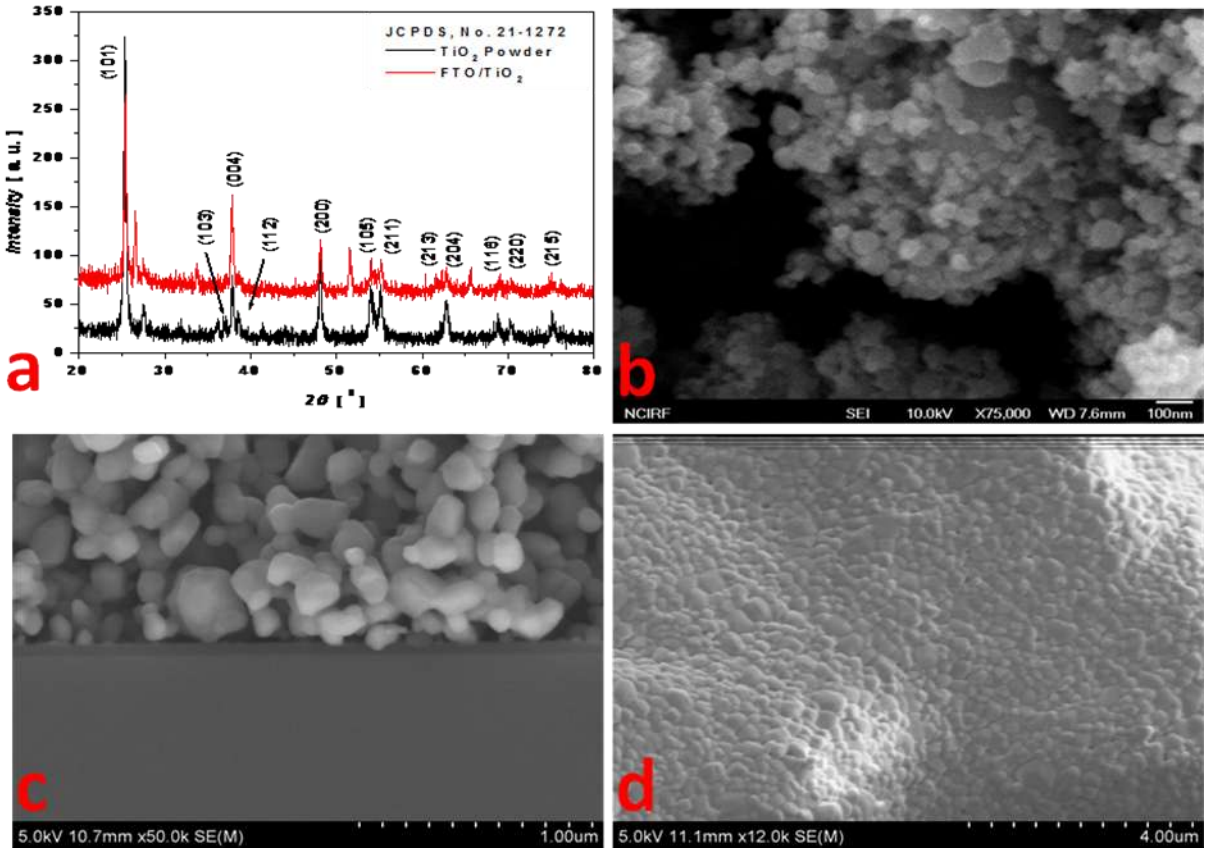

Fig.1. (a) XRD patterns of TiO_2 nanoparticles, TiO_2 coated on FTO glass, HR-SEM images of (b) TiO_2 nanoparticles, (c) Cross-section view and (d) plane view of TiO_2 coated on FTO glass.

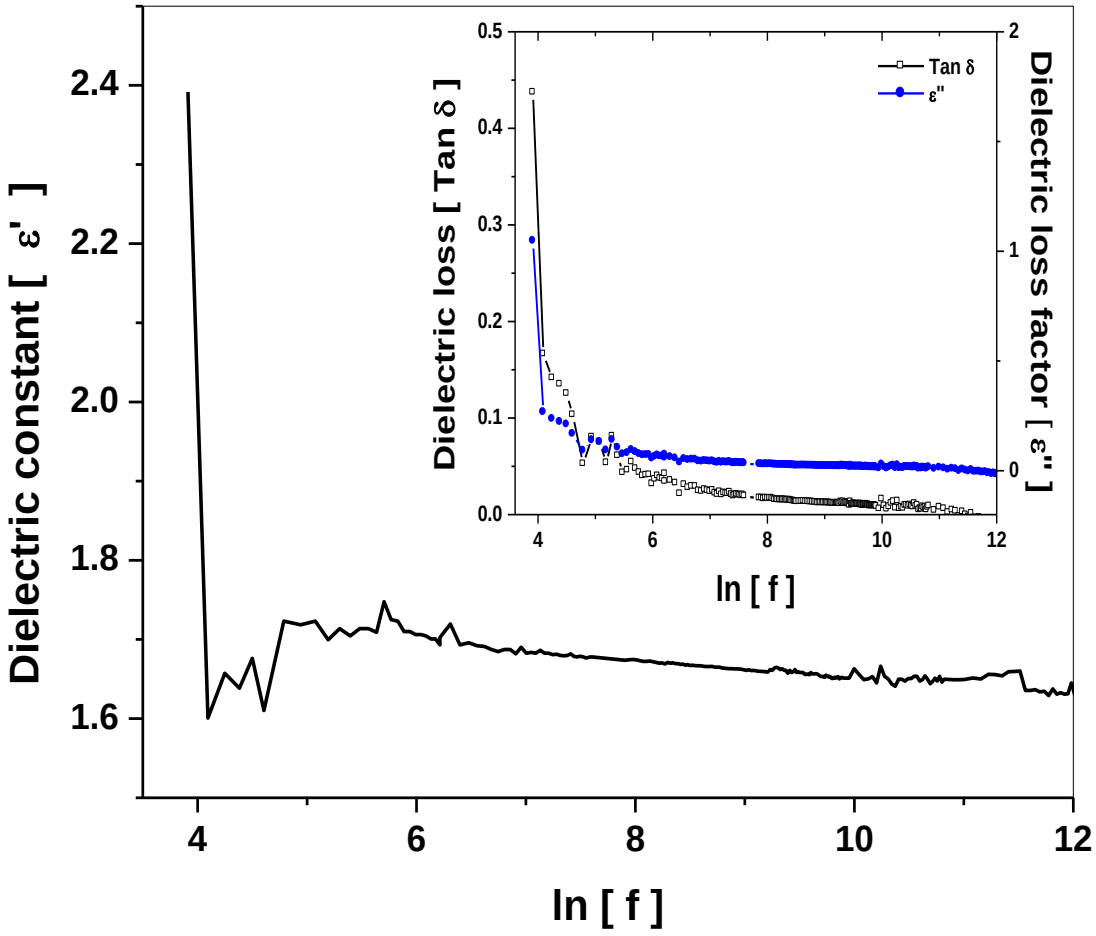

Fig.2. Variation of dielectric constant (ε') of FTO/ TiO_2 and the inset shows the variation of dielectric loss (*tan* δ) and dielectric loss factor (ε'') of FTO/ TiO_2

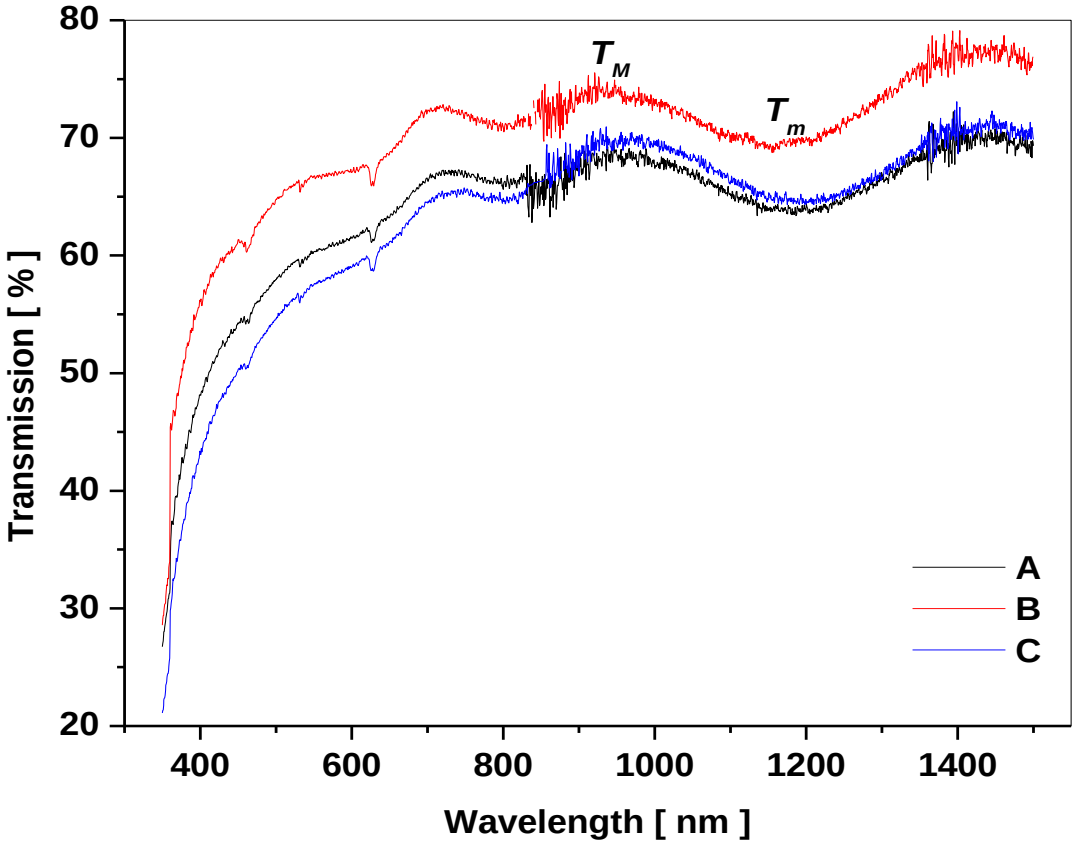

Fig.3. Transmission spectra of TiO_2 thin films deposited on FTO glass substrates.

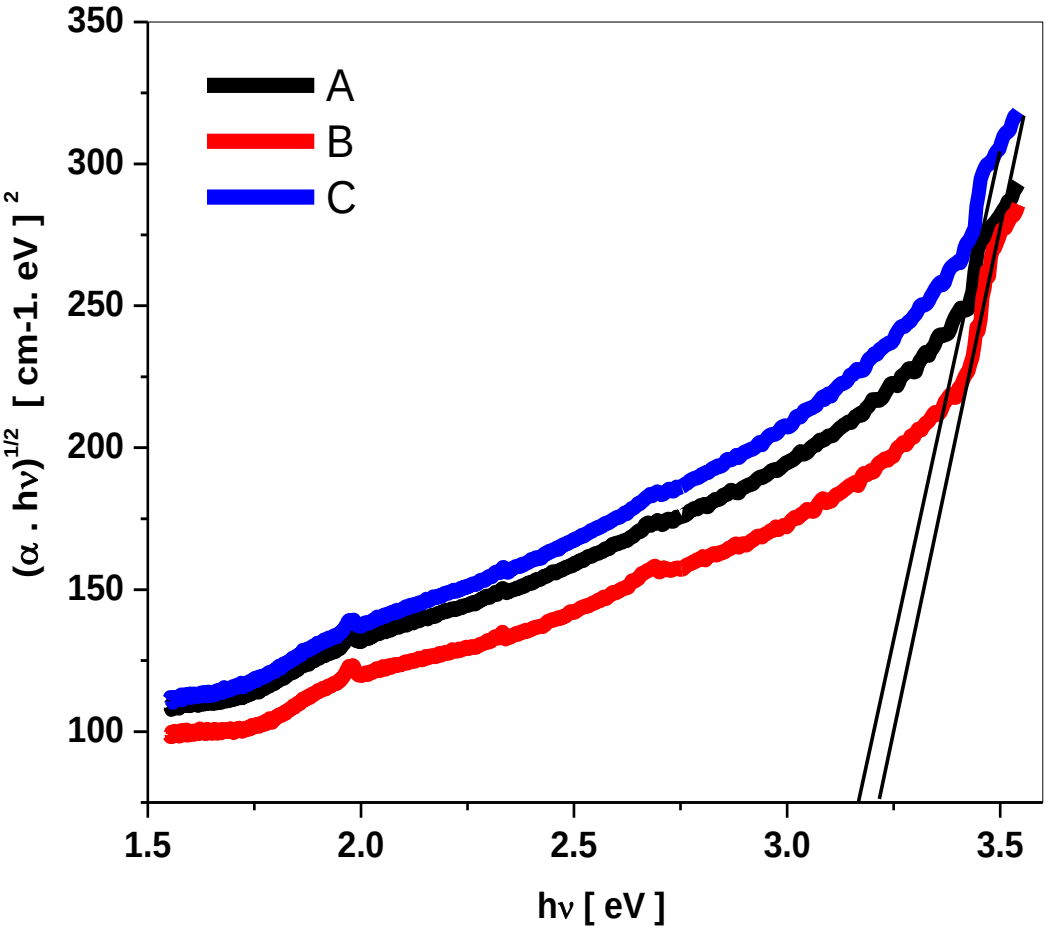

Fig.4. Tauc plots for samples A, B and C

Table 1: Values of λ_{max}, λ_{min}, τ_s, T_M, T_m, S, N, n and d, for TiO_2 thin films from transmission spectra of Figure 3.

Sample	**λ_{max}**	**λ_{min}**	**τ_s**	**T_M**	**T_m**	**S**	**N**	**n**	**d (nm)**
A	955	1202	0.8739	0.6863	0.6360	1.87	2.6794	2.14	540
B	963	1195	0.8645	0.7029	0.6425	1.92	2.8568	2.23	553
C	945	1184	0.8659	0.7354	0.6952	1.96	2.7290	2.15	544